Title

Genome-wide Profiling of Genetic Synthetic Lethality Identifies CDK12 as a Novel Determinant of PARP1/2 Inhibitor Sensitivity

Journal

Cancer Research, 74(1)

ISSN

0008-5472

Authors

Bajrami, Ilirjana
Frankum, Jessica R
Konde, Asha
et al.

Publication Date

2014

DOI

10.1158/0008-5472.can-13-2541

Peer reviewed

HHS Public Access

Author manuscript

Cancer Res. Author manuscript; available in PMC 2016 May 31.

Published in final edited form as:

Cancer Res. 2014 January 1; 74(1): 287–297. doi:10.1158/0008-5472.CAN-13-2541.

Genome-wide profiling of genetic synthetic lethality identifies CDK12 as a novel determinant of PARP1/2 inhibitor sensitivity

Ilirjana Bajrami[1,*], **Jessica R. Frankum**[1,*], **Asha Konde**[1], **Rowan E. Miller**[1], **Farah L. Rehman**[1], **Rachel Brough**[1], **James Campbell**[1,3], **David Sims**[1], **Rumana Rafiq**[1], **Sean Hooper**[1], **Lina Chen**[3], **Iwanka Kozarewa**[3], **Ioannis Assiotis**[3], **Kerry Fenwick**[3], **Rachael Natrajan**[2], **Christopher J. Lord**[1], and **Alan Ashworth**[1]

[1]CRUK Gene Function Laboratory, Breakthrough Breast Cancer Research Centre, The Institute of Cancer Research, London, SW3 6JB, UK

[2]Functional Genomics Laboratory, Breakthrough Breast Cancer Research Centre, The Institute of Cancer Research, London, SW3 6JB, UK

[3]Tumour Profiling Unit, The Institute of Cancer Research, London, SW3 6JB, UK

Abstract

Small molecule inhibitors of PARP1/2 such as olaparib have been proposed to serve as a synthetic lethal therapy for cancers that harbor *BRCA1* or *BRCA2* mutations. Indeed, in clinical trials PARP1/2 inhibitors elicit sustained anti-tumor responses in patients with germ-line *BRCA* gene mutations. In hypothesizing that additional genetic determinants might direct use of these drugs, we conducted a genome-wide synthetic lethal screen for candidate olaparib sensitivity genes. In support of this hypothesis, the set of identified genes included known determinants of olaparib sensitivity, such as BRCA1, RAD51 and Fanconi's anemia susceptibility genes. Additionally, the set included genes implicated in established networks of DNA repair, DNA cohesion and chromatin remodelling, none of which were known previously to confer sensitivity to PARP1/2 inhibition. Notably, integration of the list of candidate sensitivity genes with data from tumor DNA sequencing studies identified CDK12 deficiency as a clinically relevant biomarker of PARP1/2 inhibitor sensitivity. In models of high-grade serous ovarian cancer (HGS-OVCa), CDK12 attenuation was sufficient to confer sensitivity to PARP1/2 inhibition, suppression of DNA repair via homologous recombination and reduced expression of BRCA1. As one of only nine genes known to be mutated in HGS-OVCa, CDK12 has properties that should confirm interest in its utility as a biomarker, particularly in ongoing clinical trials of PARP1/2 inhibitors and other agents that trigger replication fork arrest.

Corresponding authors: Christopher J. Lord (; Email: Chris.Lord@icr.ac.uk) Alan Ashworth (; Email: Alan.Ashworth@icr.ac.uk)
*These authors contributed equally to this work

Conflict of interest: CJL and AA are named inventors on patents describing the use of PARP inhibitors and stand to gain as part of the ICR "Rewards to Inventors Scheme"

Author contributions: Performed experiments and analysis: All authors. Designed experiments: I.B., J.R.F., C.J.L., A.A.. Wrote manuscript: C.J.L., I.B., J.R.F., A.A.. All authors approved the final draft of the manuscript.

Competing interests: C.J.L. and A.A. are named inventors on patents describing the use of PARP inhibitors and stand to gain as part of the ICR "Rewards to Inventors Scheme".

Keywords

CDK12; PARP inhibitor; ovarian cancer; shRNA screen

Introduction

Enzymes within the PARP superfamily catalyze the polymerization of Poly(ADP-Ribose) chains on substrate proteins, using β-NAD^+ as a co-factor (PARylation). The best-studied member of this superfamily, PARP1, has a relatively well-defined role in the DNA damage response (DDR) and binds damaged DNA, PARylates DNA repair effectors such as XRCC1 and performs autoPARylation, an event which drives its release from DNA (1).

Small molecule PARP1 inhibitors, which also inhibit the homologous PARP2 enzyme (hereafter referred to as PARP1/2 inhibitors), were originally developed as chemo- and radio-sensitizing agents. These agents also elicit synthetic lethality in BRCA1 or BRCA2 deficient cells, an observation which led to their clinical assessment in patients with germ-line *BRCA1* or *BRCA2* mutations (2). In Phase 1 and 2 trials, olaparib single agent treatment has delivered significant and sustained anti-tumor responses in patients with germ-line *BRCA* mutations, without causing many of the side effects associated with standard chemotherapies. Furthermore, when used as a maintenance therapy after carboplatin treatment in patients with high-grade serous ovarian cancer (HGS-OVCa), a disease characterised by a relatively high frequency of familial and somatic *BRCA* mutations, olaparib (KuDos/AstraZeneca) has been shown to significantly improve progression free survival (PFS) when compared to a placebo and in patients with *BRCA1* or *BRCA2* mutant tumors, can reduce the time to recurrence by approximately 85% (3, 4).

So far, the genetic dissection of PARP1/2 inhibitor sensitivity has relied upon the study of single genes involved in DNA repair (5) or small subsets of genes/proteins, such as the kinome (6). To identify novel genetic determinants of PARP1/2 inhibitor sensitivity that could have an impact on the clinical development of these agents, we performed a genome-wide PARP1/2 inhibitor synthetic lethal screen. The results of this screen confirm the impact of the DDR on the cellular response to PARP1/2 inhibition and identify novel genetic determinants, such as *CDK12*, that could be used as candidate predictive biomarkers in both existing and future clinical trials.

Materials and methods

Materials

The PARP inhibitor AZD2281/Olaparib, was obtained from Selleck Chemical and paclitaxel and cisplatin were obtained from Sigma Aldrich. Drugs were used as previously described (7–9).

shRNA screen

We used the OpenBiosystems GIPZ human shRNA library. Viral pools encompassing ≈ 9500 shRNAs were used to transduce MCF7 cells with a final representation of ≈ 1000 cells

per shRNA construct (Supplementary Fig. S1C). 72 hours after infection, cells were divided into cohorts and exposed to either 1.5 μM olaparib, or DMSO for 14 days. shRNA representation in the surviving cell populations was estimated via massively parallel sequencing as described in Supplementary Materials and Methods.

Cell lines

PEO1, PEO14, OV56, COV318, COV504, SKOV3 were obtained from European Collection of Cell Cultures (ECACC). PEO1 and PEO14 cells were grown in RPMI1640 containing 2mM Glutamine, 2mM Sodium Pyruvate and 10% (v/v) Foetal Bovine Serum (FBS). OV56 cells were grown in Dulbecco's Modified Eagle Medium (DMEM):F12 Nutrient Mixture containing 2mM Glutamine, 5% (v/v) FBS, 0.5 μg/ml hydrocortisone (Sigma Aldrich) and 10μg/ml insulin (Sigma Aldrich). COV318 and COV504 cells were grown in DMEM containing 2mM Glutamine and 10% (v/v) FBS. SKOV3 cells were grown in McCoy's 5a media containing 2mM Glutamine and 15% (v/v) FBS. OV90 and CAOV3 were obtained from American Type Culture Collection (ATCC). OV90 cells were grown in a 1:1 mixture of MCDB105 containing 1.5 g/L sodium bicarbonate and Medium 199 containing 2.2 g/L sodium bicarbonate and 15% (v/v) FBS. CAOV3 cells were grown in DMEM containing 2mM Glutamine and 10% (v/v) FBS. The identity of cell lines was confirmed by STR typing using the StemElite kit (Promega) in February 2013. Cell lines were confirmed as being mycoplasma negative using the MycoAlert kit (Lonza) routinely throughout experimentation. Cell lines were transfected with SMARTpool siRNAs obtained from Dharmacon or Santa Cruz Biotech using RNAiMax (Invitrogen) transfection reagent. See also Supplementary Materials and Methods.

Protein analysis

Cells were lysed in NP250 buffer (20 mM Tris pH 7.6, 1 mM EDTA, 0.5 % NP40, 250 mM NaCl) containing protease inhibitor cocktail tablets (Roche). Protein quantification was estimated using BioRad Protein Assay Reagent (BioRad). Whole cell lysates were electrophoresed on Novex 4–12% gradient bis–tris pre-cast gels (Invitrogen) and immunoblotted overnight at 4°C with antibodies listed in Supplementary Table S1.

HR assay

A synthetic repair reporter was used as previously described (8, 10–12). HeLa cells harboring a single-copy genomic integration of the DR-GFP reporter were transfected with siRNA targeting CDK12, BRCA1, BRCA2 or a siControl. 24 hours later, cells were transfected with the I-*Sce*I expression vector, pcBASce, or an empty vector control (11). Forty-eight hours later, HR frequency was estimated by quantifying the frequency of GFP positive cells using FACS (11).

Immunohistochemistry

The quantification of nuclear RAD51 foci was performed as in (7). See also Supplementary Materials and Methods.

Quantitative RT-PCR

Quantitative RT-PCR was carried out using Assay-on-Demand primer/probe sets (Applied Biosystems). Gene expression was calculated relative to the expression of *GAPDH*, and adjusted relative to expression in shNTC infected cells.

Survival analysis

OS analysis was performed using stage-II–IV HGS-OVCa samples from the TCGA dataset (13) as described in the Supplementary Materials and Methods.

In vivo efficacy studies

In vivo efficacy study was performed using OV90 cells infected with either non-targeting shRNA (shNTC) or shCDK12 expression constructs. A detailed protocol is described in Supplementary Materials and Methods.

Results

A genome-wide synthetic lethality screen for sensitivity to a clinical PARP1/2 inhibitor

To identify determinants of PARP1/2 inhibitor response, we designed a high-throughput RNA interference (RNAi) synthetic lethality screen (Supplementary Fig. S1A). For this screen, we selected MCF7 breast tumor cells as they are *BRCA1* and *BRCA2* wild type, olaparib resistant (Supplementary Fig. S1B) and amenable to high-efficiency lentiviral infection (Supplementary Fig. S1C). Cells were infected with a GIPZ human short hairpin (sh)RNA library encompassing 57,540 lentiviral shRNA expression constructs targeting 16,487 unique human protein-coding genes (Ensembl 56). The shRNA library was divided into six pools, with each pool encompassing between 9,541–9,601 shRNAs. MCF7 cells were infected with each GIPZ pool at a multiplicity of infection of 0.8, generating ≈ 1000 infected cells per shRNA construct. This ratio of cells infected per shRNA construct was maintained throughput the experiment (Supplementary Fig. S1C). 72 hours after infection, cell populations were divided into two cohorts, one exposed to the clinical PARP1/2 inhibitor olaparib (KuDOS/AstraZeneca), the other exposed to DMSO, the olaparib vehicle. To maximize the potential for identifying synthetic lethal/sensitizing effects, cells were exposed to 1.5 μM olaparib, a concentration that caused a 20% reduction in cell survival (Surviving Fraction 80, SF_{80}, Supplementary Fig. S1B). In total, cells were exposed to olaparib or DMSO for 14 days (10 population doublings) so as to model chronic olaparib exposure as used in the clinic.

To identify shRNA constructs that modulated the response to olaparib. We estimated shRNA enrichment and depletion in cells that survived olaparib or DMSO exposure using massively parallel sequencing. In brief, genomic DNA from surviving cell populations was recovered and shRNA target sequences were PCR amplified using primer sequences compatible with Illumina GAIIx sequencing (see Supplementary Materials and Methods). PCR amplicons were sequenced on a Illumina GAIIx platform, generating >1,000 short-reads for each shRNA in the library. After aligning short-read sequences to the known sequence of shRNAs present in each pool, we used the frequency of each short-read to estimate the frequency of shRNAs in each surviving population. After data normalization to account for variation

between viral pools and replicas (see Supplementary Materials and Methods), we identified shRNA constructs that modulated the MCF7 response to olaparib by comparing the abundance of shRNA-specific short-reads in olaparib and vehicle treated cultures. Over representation of shRNA sequence in an olaparib treated sample indicated a resistance-causing effect, whereas under representation indicated a sensitization effect. These over- and under-representation effects were quantified as Drug Effect (DE) Z or Standardized Scores (See Supplementary Materials and Methods), with negative DE scores indicating sensitization effects and positive DE scores indicating resistance-causing effects (Fig. 1A–C). In total, we performed two biological replicas of the screen and calculated average DE scores for each shRNA from the replica data (Fig. 1A).

We calculated DE Z score values using the Median Absolute Deviation (MAD) and defined sensitization effects as those shRNAs that gave DE Z scores < −1.96, a threshold approximately equivalent to $p<0.05$ and likewise resistant effects as those shRNAs that gave Z score >1.96 (Fig. 1B, Supplementary Tables S2 and S3). In total, we identified 2,339 shRNA constructs targeting 2,208 different genes causing an enhancement of olaparib sensitivity in MCF7 cells and 2,043 shRNA constructs targeting 1,902 genes causing an increase in olaparib resistance. We found that of 2,208 different genes appearing in the candidate sensitivity list, the well-established PARP1/2 inhibitor sensitivity gene *BRCA1* (nine shRNAs with DE Z score <−1.96) and the *ATAD5* gene *(ATPase family, AAA domain containing 5,* four shRNAs with DE Z score <−1.96), were represented by >2 shRNAs with DE Z scores <−1.96. ATAD5 is known to modulate PCNA deubiquitination and genomic stability (16–18) and we found that silencing of *ATAD5* enhanced olaparib sensitivity and reduced RAD51 foci formation (a major determinant of PARP1/2 inhibitor sensitivity - Supplementary Fig. S2), giving us some confidence in the results of the screen. Five percent of the genes (119 genes) in the candidate sensitivity list were represented by two shRNAs with DE <−1.96 whilst the vast majority of genes in the sensitivity list were represented by one shRNA with DE < −1.96 (2,089 genes, 95 %). Similarly, in the candidate resistance-causing gene list, there were 141 genes represented by two shRNAs (7 %) and 1,761 genes (93 %) represented by one shRNA. From our experience with this shRNA library (19, 20) the predominance of hits represented by >1 shRNAs is common and explains the rationale behind efforts that many have made to increase the number of shRNA species per gene in newer generation shRNA libraries (21).

Using pathway annotation tools such as KEGG and literature sources, we annotated the list of candidate “hit” genes in order to identify the predominant known molecular networks explaining the response to olaparib. To facilitate network analysis, we annotated all genes where at least one shRNA caused either sensitivity or resistance as defined above. In the case of the olaparib sensitivity causing effects, the two most predominant networks represented were DNA repair processes and DNA cohesion/chromatin remodelling. For example, we found evidence for an involvement in DNA repair for at least 74 genes in the candidate sensitivity-causing gene list (Fig. 1D, Supplementary Fig. S3 and Supplementary Table S4). Of these, 65 % (48 genes) have already been implicated in either BRCA1 function, DNA double-stand break repair, the Fanconi Anemia pathway or HR (Fig. 1D and E, Supplementary Fig. S3 and Supplementary Table S4). Furthermore, 14 genes in the candidate sensitivity gene list have previously been reported as modulating PARP1/2

inhibitor sensitivity (*BRCA1, NBN, FANCD2, FANCC, RAD51, MCM3, CDK7, GTF2H3, LIG3, POLH, PTEN, USP1, RAD51D* and *RAD51C*, Supplementary Table S4 (6, 8, 22–25)). The identification of a series of HR genes and known PARP1/2 inhibitor sensitisation effects in our candidate hit list gave us considerable confidence in the screen data and supports the hypothesis that HR is a key determinant of PARP1/2 inhibitor sensitivity. However, we did note that some critical HR genes were not present in our candidate hit list, such as *BRCA2* and *DSS1*; it seems possible that the shRNA constructs for these genes do not cause a level of gene silencing sufficient to elicit HR deficiency, reinforcing the idea that the negative predictive value of such screens (i.e. the ability to identify genes that do not cause the phenotype of interest) might be limited.

We also noted that a number of cohesins, chromatin remodelling proteins and replication associated genes that are involved in DNA repair were found in our candidate sensitisation gene list (e.g. the cohesion-associated genes, *RAD21, ESCO1, ESCO2* and *SMC3*, the MCM protein coding genes *MCM2, 3* and *6* and the topoisomerase coding genes *TOP3A* and *TOP2B*, Fig. 1F; Supplementary Table S4, Supplementary Fig. S3) highlighting the potential impact of sister chromatid cohesion and chromatin remodelling in the response to PARP1/2 inhibitor-induced lesions. This latter observation is consistent with work identifying cohesins and associated proteins as being critical to the DDR (10, 26). In addition, a number of other DNA repair proteins not so far linked to HR were also identified in the candidate sensitisation gene list, including those involved in Base Excision Repair (BER) and Nucleotide Excision Repair (NER) (Supplementary Table S4), such as *LIG3* and *POLB* (27) (for the purposes of classification, defined as BER proteins) and *GTF2H3* and *CDK7* (both NER). Of these, *LIG3*, *GTF2H3* and *CDK7* have previously been implicated in PARP1/2 inhibitor sensitivity (23). The identification of multiple components of DDR not implicated in HR in the candidate gene list here, suggests that the response to PARP1/2 inhibitor driven DNA lesions is perhaps more complex.

Amongst the olaparib resistance causing effects, we noted that two shRNAs targeting the olaparib target *PARP1*, caused olaparib resistance with DE Z scores of 2.0 and 3.4 (Supplementary Table S3). This observation is consistent with recent work identifying *PARP1* deficiency as a cause of PARP inhibitor resistance in cells with functional HR (28, 29). It is suggested that the cytotoxic DNA lesions in cells exposed to PARP1/2 inhibitors are trapped PARP1–DNA complexes (28). These lesions most likely form as catalytic PARP inhibitors reduce PARP1 autoPARylation, an event that is normally required for the release of PARP1 from DNA. In the absence of PARP1, these DNA lesions do not form and the cytotoxicity normally caused by PARP1/2 inhibitors is reduced (28, 29).

Integration of the olaparib sensitisation profile with tumor mutation data

One of our aims in this study was to identify genetic biomarkers that could be used to inform the clinical use of PARP1/2 inhibitors. Already, a number of cancer-associated mutations predict sensitivity to PARP1/2 inhibitors, such as loss of function mutations in *BRCA1* and *BRCA2*. To identify other loss of function cancer mutations that could predict sensitivity to olaparib, we integrated our list of candidate shRNA sensitivity effects with publically available data describing somatic and germ-line mutations in a range of cancer histologies

(30–32). As predicted, this analysis highlighted the presence of recurrent cancer-associated mutations in known olaparib sensitisation genes identified in our shRNA screen, such as *BRCA1, ATM, FANCD2, FANCE* and *PTEN. CDK12* (ENSG00000167258, also known as *CRK7, CRKR, CRKRS*), a gene represented in the olaparib shRNA sensitization list (DE = −4.3, Supplementary Table S2) was identified as one of only nine genes found to be significantly mutated in HGS-OVCa (13). In a recent genomic analysis of 316 HGS-OV tumors, nine tumors were found to have somatic *CDK12* mutations (3%); in the same dataset *BRCA1* and *BRCA2* were found to be mutated in 12 % (*BRCA1*) and 11 % (*BRCA2*) of tumors (13). Five of the *CDK12* mutations in HGS-OVCa were nonsense or insertion/deletion mutations likely to be loss of function mutations (Fig. 2A and Supplementary Table S5). Furthermore, as Spellman and colleagues noted, the additional four missense *CDK12* mutations identified in HGS-OVCa clustered in the protein kinase coding domain of CDK12, suggesting that they could compromise kinase activity (13). A subsequent analysis of the variant allele frequency of *CDK12* mutations in HGS-OVCa has also suggested that loss of the wild type *CDK12* allele occurs in the majority of *CDK12* mutant tumors, further arguing the case for *CDK12* as an HGS-OVCa tumor suppressor gene (33). By analysing data from the TCGA study describing the mutational spectrum of HGS-OVCa (13), we found that in 95 % of *BRCA1* mutations (36/38 cases) were mutually exclusive with mutations in *BRCA2*, an expected observation given the involvement of these two genes in a common pathway (HR) (13). We also found that the majority of *CDK12* mutations in this same data set (78 %, 7/9 cases) were mutually exclusive with mutations in either *BRCA1* or *BRCA2* (Fig 2B). Although the mutual exclusivity relationships between *BRCA1*, *BRCA2* and *CDK12* mutations were not complete (i.e. 100 %) the distribution of mutations in these three genes across the TCGA dataset may represent an alternative means to confer the same phenotype suggesting epistasis or a common pathway being compromised.

CDK12 and PARP1/2 inhibitor sensitivity

The appearance of CDK12 in our olaparib sensitization gene list, alongside the *CDK12* mutational data, suggested the possibility that loss of CDK12 function could sensitize tumor cells to PARP1/2 inhibitors and that loss of CDK12 function in HGS-OVCa could be a predictive biomarker for response to this developmental class of agents.

To test this, we first assessed the olaparib sensitivity of a panel of HGS-OVCa cell line models using the gold-standard clonogenic assay format, exposing cells to olaparib for two weeks. This analysis demonstrated a gradation of response from the sensitive PEO1 (hemizygous *BRCA2* p.Y1655X mutant, (34)) model through to the resistant SKOV3 cell line (Fig. 3A and Table 1). Next generation sequencing of most of these models has not identified *CDK12* mutations (35), however, by performing RT-PCR and western blot analysis of CDK12 across the tumor cell line panel (Fig. 3B and C), we found a significant correlation between reduced *CDK12* expression and olaparib sensitivity (Fig. 3B and D, $p<0.05$, Students t-test).

To directly assess the relationship between CDK12 deficiency and PARP1/2 inhibitor sensitivity, we silenced CDK12 in the profoundly olaparib resistant OV90 ovarian cancer

cell line and assessed olaparib sensitivity. Three different CDK12 shRNA lentiviral constructs caused partial silencing of CDK12 (Fig. 4A and B) and a modest yet significant increase in olaparib sensitivity (Fig. 4C, $p<0.05$, ANOVA), at a scale equivalent to that achieved by a shRNA construct targeting BRCA1. In addition, a siRNA targeting CDK12 also sensitized OV90 cells to olaparib (Fig. 4D, $p<0.001$, ANOVA). Moreover, shRNA targeting CDK12 also sensitized an additional HGS-OVCa model, PEO14 to olaparib (Supplementary Fig. S4A and B, $p<0.05$, ANOVA), suggesting the generality of this effect. We analysed whether restoring CDK12 expression could confer PARP1/2 inhibitor resistance in a tumor cell line with low levels of endogenous CDK12 expression, such as CAOV3. Ectopic expression of CDK12 significantly restored olaparib resistance (Supplementary Fig. S4C, $p<0.05$, ANOVA for CDK12 cDNA expression construct vs a control (empty vector) cDNA expression construct). Sensitivity to the microtubule poison paclitaxel was not increased by CDK12 silencing (Supplementary Fig. S4D), suggesting that CDK12 dysfunction does not in general confer sensitivity to cancer drugs.

We also assessed the hypothesis that the relationship between CDK12 dysfunction and PARP1/2 inhibitor sensitivity could be explained by a reduction of HR, the predominant pathway identified in our PARP1/2 inhibitor synthetic lethality screen (Supplementary Fig. S3). To assess this, we measured HR activity using a synthetic DNA HR substrate (DR-GFP) that generates a GFP signal once an experimentally induced DNA double strand break (DSB) has been repaired by HR (11, 12). HeLa cells harbouring the DR-GFP reporter system were reverse transfected with siRNA targeting CDK12, BRCA1, or BRCA2 and 24 hours later, a single DSB was introduced in the synthetic DNA substrate via the expression of the I*Sce*1 restriction endonuclease (11). CDK12 silencing caused a 70% reduction in HR, a level of suppression similar to that caused by siRNA targeting BRCA1 or BRCA2 (Fig. 5A, $p<0.0001$, Students t-test). We also assessed another marker of HR, the ability to form nuclear RAD51 foci in response to DNA damage (5). Silencing of CDK12 resulted in a significant reduction in ionizing radiation induced RAD51 foci formation, when compared to control treated cells (Fig. 5B and C, $p<0.001$, Students t-test), an observation consistent with the DR-GFP data and supporting the hypothesis that the modulation of PARP1/2 inhibitor sensitivity via reduced CDK12 activity is mediated by a defect in HR.

Blazek and colleagues recently reported that CDK12 dysfunction results in a reduction in expression of key DNA repair proteins such as BRCA1, FANCI, FANCD2 and ATR, as well as sensitivity to chemotherapies that stall replication forks such as mitomycin C and camptothecin (36). We found that *CDK12* silencing in two HGS-OVCa models also caused sensitivity to the replication fork stalling agent cisplatin ($p<0.001$, ANOVA for each CDK12 shRNA vs. a non-targeting control (shNTC) Supplementary Fig. S4E and F). In the first instance we tested whether mRNA transcript levels of *BRCA1*, *FANCD2*, *ATR* and *FANCI* were regulated by CDK12 in HGS-OVCa cells infected with CDK12 shRNAs (Supplementary Fig. S5A). We noted that levels of BRCA1 mRNA and protein were reduced by two different CDK12 shRNA expression constructs, whilst levels of other DNA repair proteins, such as ATR, were not (Fig. 5D, E and Supplementary Fig. S5A and B, $p<0.05$, Student's t-test). The suppression of this key HR gene (*BRCA1*) provides a possible mechanistic explanation for the HR dysfunction and PARP1/2 inhibitor sensitivity seen in CDK12 defective cells. As HR and PARP1/2 inhibitor resistance can be restored in BRCA1

deficient cells by loss of 53BP1 activity (37–39) and BRCA1 levels were reduced by CDK12 suppression (Fig. 5D and E), we tested the possibility that inhibition of 53BP1 could also restore PARP1/2 inhibitor resistance in the absence of CDK12 expression. Gene silencing of 53BP1 in combination with silencing of CDK12 (Supplementary Fig. S5C) caused a modest increase in olaparib resistance (Fig. 5F, $p<0.0001$, Student's t-test), consistent with the hypothesis that the loss of BRCA1 expression could play some role in mediating PARP1/2 inhibitor sensitivity in HGS-OVCa tumor cells with low CDK12. CCNK (also known as Cyclin K) is the cyclin partner of CDK12 and regulates CDK12 expression (36). Using a previously validated RNA interference reagent for CCNK (36), we established that targeting of CCNK, also caused olaparib and cisplatin sensitisation in a HGS-OvCa model, at a scale equivalent to that achieved by CDK12 silencing (Supplementary Fig. S6A and B).

Given the data suggesting the role of CDK12 in HR, we sought to determine whether the extent of tumor *CDK12* mRNA expression correlated with response to platinum therapy. Using survival data from patients treated with platinum therapy in the recent TCGA study, where corresponding tumor mRNA levels were also quantified (13), we found that the patients with the lowest levels of tumor *CDK12* mRNA expression had improved overall survival (OS) compared to those with elevated levels of *CDK12* mRNA (Fig. 6A, $p=0.0076$ (Log-rank Test), hazard ratio (HR) = 0.55, and Fig. 6B, $p=0.0375$ (Student's t-test)). Of note, the patients with tumor *CDK12* mutations predicted to be most deleterious to *CDK12* function (i.e. truncating mutations such p.L122fs, p.Q602*, p.W719* and p.L926fs) fell into the *CDK12* "low" cohort in this analysis.

On the basis of this preliminary clinical data, we assessed the therapeutic effect of olaparib on CDK12 deficient tumor cells *in vivo*. OV90 cells stably expressing a CDK12 shRNA expression construct (shCDK12+ve) or a control, non-targeting (shNTC+ve) shRNA construct were subcutaneously xenografted into female athymic nude mice. Once tumors had established and were measurable, mice were randomized into one of four treatment groups: (i) a shCDK12+ve OV90 xenograft bearing cohort treated with vehicle, (ii) a shCDK12+ve OV90 xenograft bearing cohort treated with olaparib, (iii) a shNTC+ve OV90 xenograft bearing cohort treated with vehicle, and (iv) a shNTC+ve OV90 xenograft bearing cohort treated with olaparib. There was a clear and statistically significant inhibitory effect of olaparib on tumor volume in shCDK12+ve tumor xenografts compared to the other cohorts (Fig. 6C and D, $p<0.001$, ANOVA for the shCDK12+ve olaparib treated cohort vs. each other cohort; all other comparisons returned a non significant p-value). The treatment regime was well tolerated, with none of the mice showing a significant change in body weight (Supplementary Fig. S6).

Discussion

As far as we are aware, this is the first attempt to define on a genome-wide scale the compendium of genes that controls the cellular response to a clinical PARP1/2 inhibitor. The initial analysis of this data confirms that the status of the DNA damage response apparatus and particularly, HR, is a key factor in determining the cytotoxicity of olaparib. Furthermore, genes that control chromatin remodelling and sister chromatid cohesion, perhaps as part of

the DDR, also seem to modulate the response to olaparib. Subsequent interrogation of the compendium of candidate PARP1/2 inhibitor genes generated in this study could in future identify additional molecular networks that explain how cells respond to these drugs.

One of the major issues in the clinical development of PARP1/2 inhibitors is the identification of biomarkers other than *BRCA1* and *BRCA2* gene mutations that predict a favourable response to therapy. For example, Phase I and II studies established that olaparib could be administered safely and that it showed significant responses in germ-line *BRCA*-mutation carriers with breast, ovarian or prostate tumors. However, not all trials have been so positive; efforts to target patient subgroups without germ-line *BRCA* mutations but which might have similar HR defects, such as triple negative breast cancers have not met with similar success (40). Similarly, the mixed responses to olaparib in patients with HGS-OVCa (4), a patient subgroup selected for trial because of its presumed high frequency of tumor specific HR defects, argues the case for the identification of additional biomarkers that could be used to direct the use of PARP1/2 inhibitors. We propose that *CDK12* should be considered as a candidate PARP1/2 inhibitor response biomarker and assessed in additional patient material from existing PARP1/2 inhibitor trials and integrated into the design of future trials, especially given its recurrent mutation in HGS-OVCa.

One future use of the compendium of genes described here is in the development of metagenes that predict the response to therapy. For example, we, and others, have previously shown that aggregate measures of gene expression from groups or modules of genes (metagenes) identified in functional profiling studies can correlate with patient responses (19). Once the full panoply of genomic and transcriptomic profiling of tumors from patients on PARP1/2 inhibitor trials becomes available, such analyses may become possible. Of course, such an approach should take into account the limitations of such *in vitro* genetic screens. In this particular case, we note that the screen was carried out in one tumor cell model and that cellular responses (and the genes that control these responses) may differ from cell line to cell line. Furthermore, the shRNA library used here could be improved by increasing the number of different shRNA constructs per gene and/or improving the ability of each construct to silence its target gene; both of these improvements could decrease the false positive rate, and enhance the overall quality of the data. Carrying out genetic screens such as this in an *in vivo* setting could also enhance the modelling of the tumor response within a more physiological setting.

Supplementary Material

Refer to Web version on PubMed Central for supplementary material.

Acknowledgments

This work was funded by Breakthrough Breast Cancer, Cancer Research UK, the European Union (EUROCAN and DDR projects) and the AACR (SU2C Breast Cancer Dream Team).

Funding. Breakthrough Breast Cancer (CTR-Q3-Y1), Cancer Research UK (C347/A8363), EUROCAN (HEALTH-FP7-2010-260791), DDR (HEALTH-FP7-2010-25989), AACR (1559-G-MD204).

References

1. De Vos M, Schreiber V, Dantzer F. The diverse roles and clinical relevance of PARPs in DNA damage repair: current state of the art. Biochem Pharmacol. 2012; 84:137–46. [PubMed: 22469522]
2. Lord CJ, Ashworth A. The DNA damage response and cancer therapy. Nature. 2012; 481:287–94. [PubMed: 22258607]
3. Ledermann JHP, Gourley C, Friedlander M, Vergote I, Rustin G, et al. Olaparib maintenance therapy in patients with platinum-sensitive relapsed serous ovarian cancer (SOC) and a BRCA mutation (BRCAm). ASCO: J Clin Oncol. 2013; 31:5505.
4. Ledermann J, Harter P, Gourley C, Friedlander M, Vergote I, Rustin G, et al. Olaparib maintenance therapy in platinum-sensitive relapsed ovarian cancer. N Engl J Med. 2012; 366:1382–92. [PubMed: 22452356]
5. McCabe N, Turner NC, Lord CJ, Kluzek K, Bialkowska A, Swift S, et al. Deficiency in the repair of DNA damage by homologous recombination and sensitivity to poly(ADP-ribose) polymerase inhibition. Cancer Res. 2006; 66:8109–15. [PubMed: 16912188]
6. Turner NC, Lord CJ, Iorns E, Brough R, Swift S, Elliott R, et al. A synthetic lethal siRNA screen identifying genes mediating sensitivity to a PARP inhibitor. EMBO J. 2008; 27:1368–77. [PubMed: 18388863]
7. Farmer H, McCabe N, Lord CJ, Tutt AN, Johnson DA, Richardson TB, et al. Targeting the DNA repair defect in BRCA mutant cells as a therapeutic strategy. Nature. 2005; 434:917–21. [PubMed: 15829967]
8. Mendes-Pereira AM, Martin SA, Brough R, McCarthy A, Taylor JR, Kim JS, et al. Synthetic lethal targeting of PTEN mutant cells with PARP inhibitors. EMBO Mol Med. 2009; 1:315–22. [PubMed: 20049735]
9. Edwards SL, Brough R, Lord CJ, Natrajan R, Vatcheva R, Levine DA, et al. Resistance to therapy caused by intragenic deletion in BRCA2. Nature. 2008; 451:1111–5. [PubMed: 18264088]
10. Brough R, Bajrami I, Vatcheva R, Natrajan R, Reis-Filho JS, Lord CJ, et al. APRIN is a cell cycle specific BRCA2-interacting protein required for genome integrity and a predictor of outcome after chemotherapy in breast cancer. EMBO J. 2012; 31:1160–76. [PubMed: 22293751]
11. Saeki H, Siaud N, Christ N, Wiegant WW, van Buul PP, Han M, et al. Suppression of the DNA repair defects of BRCA2-deficient cells with heterologous protein fusions. Proc Natl Acad Sci U S A. 2006; 103:8768–73. [PubMed: 16731627]
12. Pierce AJ, Johnson RD, Thompson LH, Jasin M. XRCC3 promotes homology-directed repair of DNA damage in mammalian cells. Genes Dev. 1999; 13:2633–8. [PubMed: 10541549]
13. TCGA. Integrated genomic analyses of ovarian carcinoma. Nature. 2011; 474:609–15. [PubMed: 21720365]
14. Cerami E, Gao J, Dogrusoz U, Gross BE, Sumer SO, Aksoy BA, et al. The cBio cancer genomics portal: an open platform for exploring multidimensional cancer genomics data. Cancer Discov. 2012; 2:401–4. [PubMed: 22588877]
15. Gao J, Aksoy BA, Dogrusoz U, Dresdner G, Gross B, Sumer SO, et al. Integrative analysis of complex cancer genomics and clinical profiles using the cBioPortal. Sci Signal. 2013; 6:pl1. [PubMed: 23550210]
16. Lee KY, Yang K, Cohn MA, Sikdar N, D'Andrea AD, Myung K. Human ELG1 regulates the level of ubiquitinated proliferating cell nuclear antigen (PCNA) through Its interactions with PCNA and USP1. J Biol Chem. 2010; 285:10362–9. [PubMed: 20147293]
17. Sikdar N, Banerjee S, Lee KY, Wincovitch S, Pak E, Nakanishi K, et al. DNA damage responses by human ELG1 in S phase are important to maintain genomic integrity. Cell Cycle. 2009; 8:3199–207. [PubMed: 19755857]
18. Bell DW, Sikdar N, Lee KY, Price JC, Chatterjee R, Park HD, et al. Predisposition to cancer caused by genetic and functional defects of mammalian Atad5. PLoS Genet. 2011; 7:e1002245. [PubMed: 21901109]
19. Mendes-Pereira AM, Sims D, Dexter T, Fenwick K, Assiotis I, Kozarewa I, et al. Genome-wide functional screen identifies a compendium of genes affecting sensitivity to tamoxifen. Proc Natl Acad Sci U S A. 2012; 109:2730–5. [PubMed: 21482774]

20. Sims D, Mendes-Pereira AM, Frankum J, Burgess D, Cerone MA, Lombardelli C, et al. High-throughput RNA interference screening using pooled shRNA libraries and next generation sequencing. Genome Biol. 2011; 12:R104. [PubMed: 22018332]
21. Bassik MC, Lebbink RJ, Churchman LS, Ingolia NT, Patena W, LeProust EM, et al. Rapid creation and quantitative monitoring of high coverage shRNA libraries. Nat Methods. 2009; 6:443–5. [PubMed: 19448642]
22. Loveday C, Turnbull C, Ramsay E, Hughes D, Ruark E, Frankum JR, et al. Germline mutations in RAD51D confer susceptibility to ovarian cancer. Nat Genet. 2011; 43:879–82. [PubMed: 21822267]
23. Lord CJ, McDonald S, Swift S, Turner NC, Ashworth A. A high-throughput RNA interference screen for DNA repair determinants of PARP inhibitor sensitivity. DNA Repair (Amst). 2008; 7:2010–9. [PubMed: 18832051]
24. Min A, Im SA, Yoon YK, Song SH, Nam HJ, Hur HS, et al. RAD51C-Deficient Cancer Cells Are Highly Sensitive to the PARP Inhibitor Olaparib. Mol Cancer Ther. 2013; 12:865–77. [PubMed: 23512992]
25. Murai J, Yang K, Dejsuphong D, Hirota K, Takeda S, D'Andrea AD. The USP1/UAF1 complex promotes double-strand break repair through homologous recombination. Mol Cell Biol. 2011; 31:2462–9. [PubMed: 21482670]
26. Wu N, Yu H. The Smc complexes in DNA damage response. Cell Biosci. 2012; 2:5. [PubMed: 22369641]
27. Horton JK, Wilson SH. Predicting enhanced cell killing through PARP inhibition. Mol Cancer Res. 2013; 11:13–8. [PubMed: 23193155]
28. Murai J, Huang SY, Das BB, Renaud A, Zhang Y, Doroshow JH, et al. Trapping of PARP1 and PARP2 by Clinical PARP Inhibitors. Cancer Res. 2012; 72:5588–99. [PubMed: 23118055]
29. Pettitt SJ, Rehman FL, Bajrami I, Brough R, Wallberg F, Kozarewa I, et al. A Genetic Screen Using the PiggyBac Transposon in Haploid Cells Identifies Parp1 as a Mediator of Olaparib Toxicity. PLoS One. 2013; 8:e61520. [PubMed: 23634208]
30. TCGA. https://tcga-data.nci.nih.gov/tcga/
31. COSMIC. http://www.sanger.ac.uk/genetics/CGP/cosmic/
32. ICGC. http://icgc.org/
33. Carter SL, Cibulskis K, Helman E, McKenna A, Shen H, Zack T, et al. Absolute quantification of somatic DNA alterations in human cancer. Nat Biotechnol. 2012; 30:413–21. [PubMed: 22544022]
34. Sakai W, Swisher EM, Jacquemont C, Chandramohan KV, Couch FJ, Langdon SP, et al. Functional restoration of BRCA2 protein by secondary BRCA2 mutations in BRCA2-mutated ovarian carcinoma. Cancer Res. 2009; 69:6381–6. [PubMed: 19654294]
35. CCLE. http://www.broadinstitute.org/ccle/home
36. Blazek D, Kohoutek J, Bartholomeeusen K, Johansen E, Hulinkova P, Luo Z, et al. The Cyclin K/Cdk12 complex maintains genomic stability via regulation of expression of DNA damage response genes. Genes Dev. 2011; 25:2158–72. [PubMed: 22012619]
37. Bunting SF, Callen E, Wong N, Chen HT, Polato F, Gunn A, et al. 53BP1 inhibits homologous recombination in Brca1-deficient cells by blocking resection of DNA breaks. Cell. 2010; 141:243–54. [PubMed: 20362325]
38. Bouwman P, Aly A, Escandell JM, Pieterse M, Bartkova J, van der Gulden H, et al. 53BP1 loss rescues BRCA1 deficiency and is associated with triple-negative and BRCA-mutated breast cancers. Nat Struct Mol Biol. 2010; 17:688–95. [PubMed: 20453858]
39. Jaspers JE, Kersbergen A, Boon U, Sol W, van Deemter L, Zander SA, et al. Loss of 53BP1 causes PARP inhibitor resistance in Brca1-mutated mouse mammary tumors. Cancer Discov. 2013; 3:68–81. [PubMed: 23103855]
40. Gelmon KA, Tischkowitz M, Mackay H, Swenerton K, Robidoux A, Tonkin K, et al. Olaparib in patients with recurrent high-grade serous or poorly differentiated ovarian carcinoma or triple-negative breast cancer: a phase 2, multicentre, open-label, non-randomised study. Lancet Oncol. 2011; 12:852–61. [PubMed: 21862407]

41. Franceschini A, Szklarczyk D, Frankild S, Kuhn M, Simonovic M, Roth A, et al. STRING v9.1: protein-protein interaction networks, with increased coverage and integration. Nucleic Acids Res. 2013; 41:D808–15. [PubMed: 23203871]

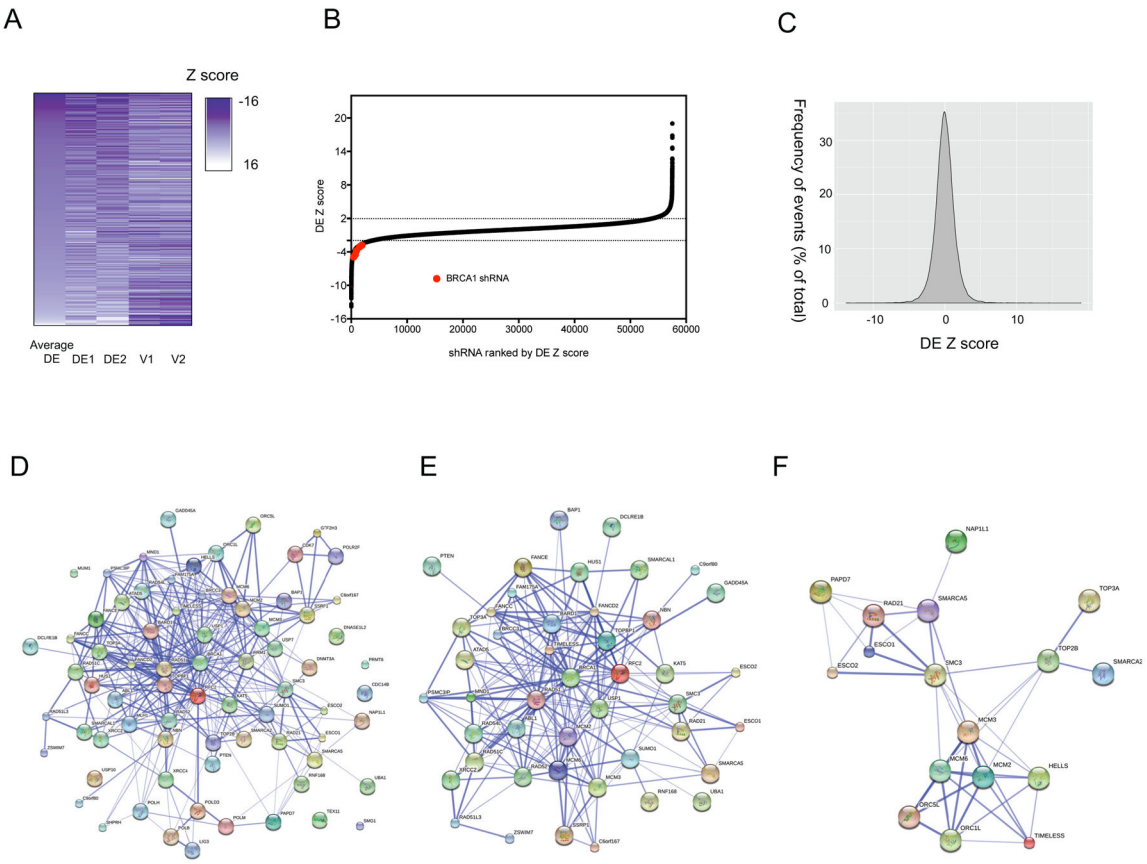

Figure 1. Genome-wide shRNA screen for the detection of olaparib sensitization effects

A, Heatmap showing the clustering of Drug Effect (DE) and Viability (V) Z scores from replica olaparib sensitization shRNA screens. The heatmap depicts DE and V Z scores for two replica screens (e.g. DE1 and V1 for replica 1 and DE2 and V2 for replica screen 2 and the average DE Z score). **B**, Plot of average olaparib DE Z scores for each of the shRNA constructs in the library. Each shRNA is ranked by its average DE Z score. DE Z score thresholds of −1.96 and 1.96 are shown as broken lines and BRCA1 shRNAs are highlighted in red. **C**, Histogram of average DE Z scores for each shRNA construct in the library. **D, E and F,** Molecular networks causing PARP1/2 inhibitor sensitivity. **D**, DNA repair genes, **E**, HR-associated genes and **F**, Cohesin and chromatin remodelling associated genes. Each gene in each network is represented by at least one shRNA with DE Z score <−1.96. Blue lines represent known physical or functional interactions between genes/proteins; dark blue lines represent high confidence interactions, with light blue lines representing less well-established interactions. Network diagrams were created from data in Supplementary Table 2, using STRING (41).

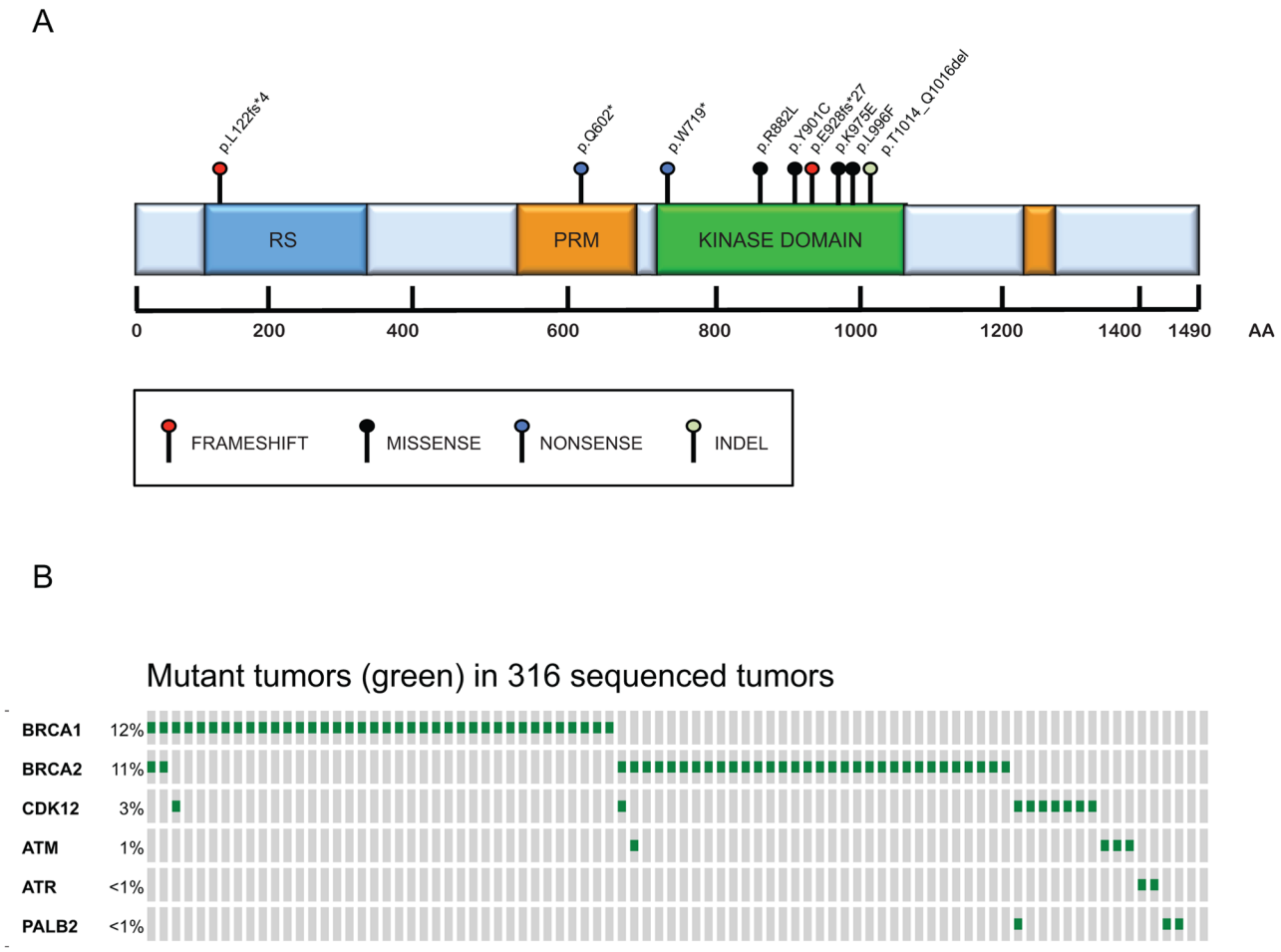

Figure 2. Mutations in *CDK12*

A, Schematic diagram of CDK12 annotated with protein alterations of CDK12 mutations in HGS-OVCa (31). Arginine/serine-rich (RS), proline-rich (PRM), kinase domain (KD) domains are indicated by blue, orange, green, respectively. Numbers below the schemes indicate the amino acid (AA) position. Coding alterations are colored as either black (missense), red (frameshift), green (indel) and blue (nonsense). Mutations in other cancer histologies are described in Supplementary Table S5. **B**, Heatmap representation of tumor-associated somatic mutations found in BRCA1, BRCA2 and CDK12 in 316 patients with HGS-OVCa, using data from (13). Each tumor is represented by a bar, with each green bar indicating a mutant tumor. Not all 316 tumors in the study cohort are shown. Frequency of gene mutations in this cohort is shown.

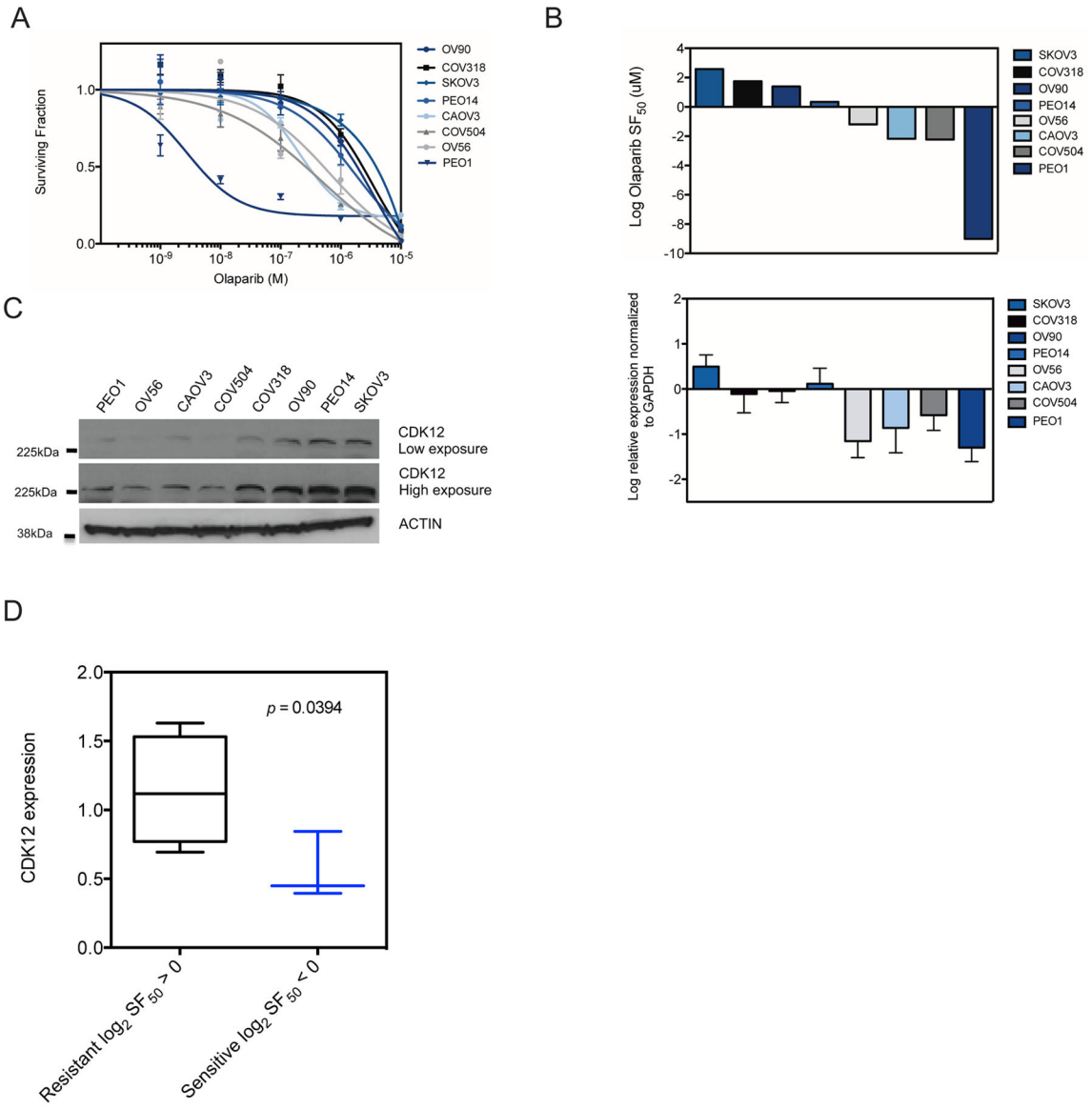

Figure 3. Low *CDK12* expression correlates with PARP1/2 inhibitor sensitivity in serous ovarian tumor cell lines

A, 14 day olaparib survival curves of serous ovarian tumor cell lines are shown. Error bars represent SEM from three independent experiments. PEO1, which harbors a hemizygous *BRCA2* p.Y1655X mutation, is included as a positive control **B,** (top panel) $\log_2$ transformed olaparib SF_{50} values for serous ovarian cancer cell line models and (bottom panel) $\log_2$ transformed *CDK12* mRNA expression levels in the same panel of serous ovarian cancer cell lines. Error bars represent SEM from triplicate independent experiments. **C,** Western blot of CDK12 expression in whole cell lysates from the tumor cell lines described in (B). ACTIN expression is shown as the loading control. **D,** Box and whiskers plot illustrating the difference in *CDK12* mRNA expression between olaparib resistant ($\log_2$ SF_{50}>0 M, n= 4 cell lines) and sensitive ($\log_2$ SF_{50}<0 M, n= 3 cell lines) serous ovarian tumor cell models, PEO1 cell line was excluded from this analysis on account of its BRCA2

mutation. *CDK12* mRNA expression is significantly lower in the sensitive cohort ($p<0.05$, Student's t-test).

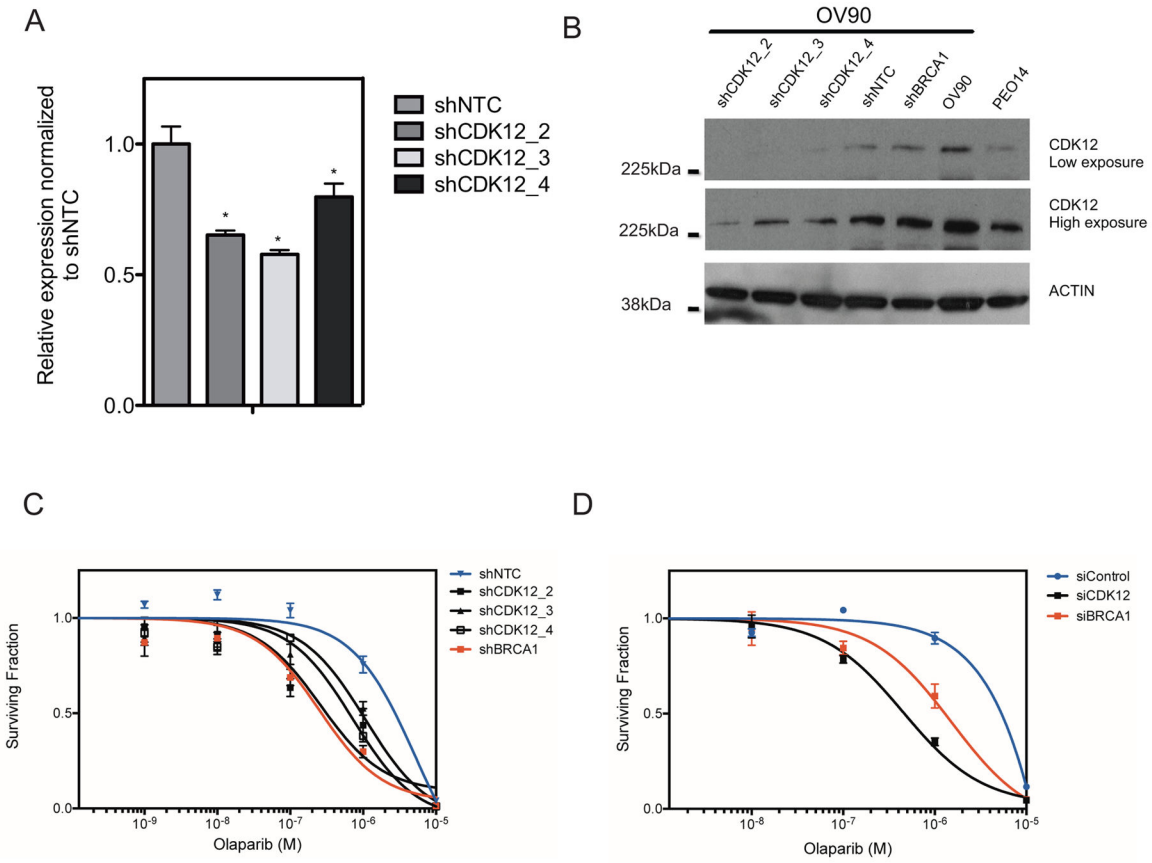

Figure 4. Silencing of CDK12 sensitises serous ovarian tumor cells to olaparib

A, Bar chart indicating *CDK12* mRNA levels in OV90 cells expressing different CDK12 shRNA expression constructs (shCDK12_2, 3 and 4) or a control, non-targeting (shNTC) shRNA construct. Error bars represent SEM from three independent measurements. Each CDK12 shRNA significantly suppressed CDK12 mRNA levels compared to shNTC, (p<0.05, Student's t test). **B,** Western blot of CDK12 expression in OV90 cells described in (A). The level of ACTIN expression was used as a loading control. **C,** 14 day olaparib survival curves of cells shown in (A). Error bars represent the SEM from three independent experiments. Each CDK12 shRNA significantly sensitised OV90 cells to olaparib compared to the shNTC population (p<0.05, ANOVA in each case). **D,** 14 day olaparib survival curves of OV90 cells transfected with a control non-targeting siRNA (siControl) or siRNAs targeting either CDK12 or BRCA1. Error bars represent the SEM from three independent experiments. CDK12 siRNA silenced OV90 cells sensitized to olaparib (p<0.05, ANOVA).

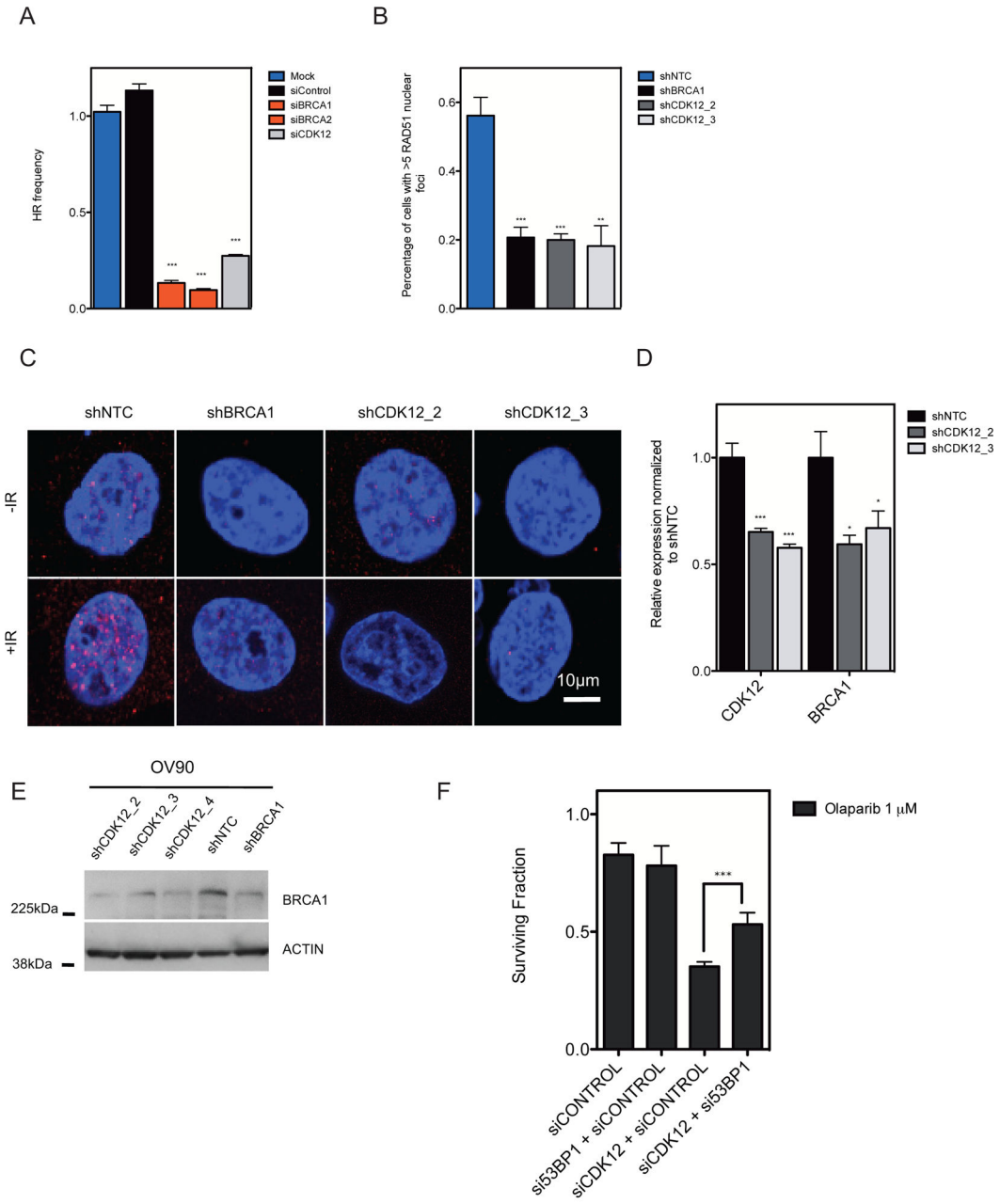

Figure 5. Silencing of CDK12 suppresses homologous recombination

A, Bar chart showing the effect of CDK12, BRCA1, BRCA2 siRNA silencing on HR frequency in HeLa cells harboring a single-copy genomic DR-GFP reporter. Error bars represent SEM from three independent experiments. CDK12 silencing significantly reduced HR frequency (***p<0.0001, Student's t-test). **B,** Bar chart illustrating the frequency of nuclear RAD51 foci in OV90 cells expressing CONTROL, BRCA1 or CDK12 shRNA after exposure to ionizing radiation. Silencing of CDK12 significantly reduced RAD51 focus formation, (**p<0.001, Students t-test). Error bars for each individual experiment represent SEM. **C**, Representative confocal microscopy images of nuclear RAD51 foci (red) of OV90

cells as in (B). **D,** Bar chart illustrating CDK12 silencing caused a significant reduction in *CDK12* and *BRCA1* expression at the mRNA level (*p<0.05 and ***p<0.001, Student t-test). Error bars represent SEM from three independent measurements. **E**, Western blot of BRCA1 expression using whole cell lysates also analysed in Fig 4B. OV90 cells expressing CONTROL, BRCA1 or CDK12 shRNA were western blotted and probed for BRCA1 or ACTIN. **F**, Surviving fractions at 1μM olaparib in OV90 cells transfected with CONTROL, CDK12 or 53BP1 siRNAs (***p<0.001, Student t-test). Error bars represent SEM from three independent experiments.

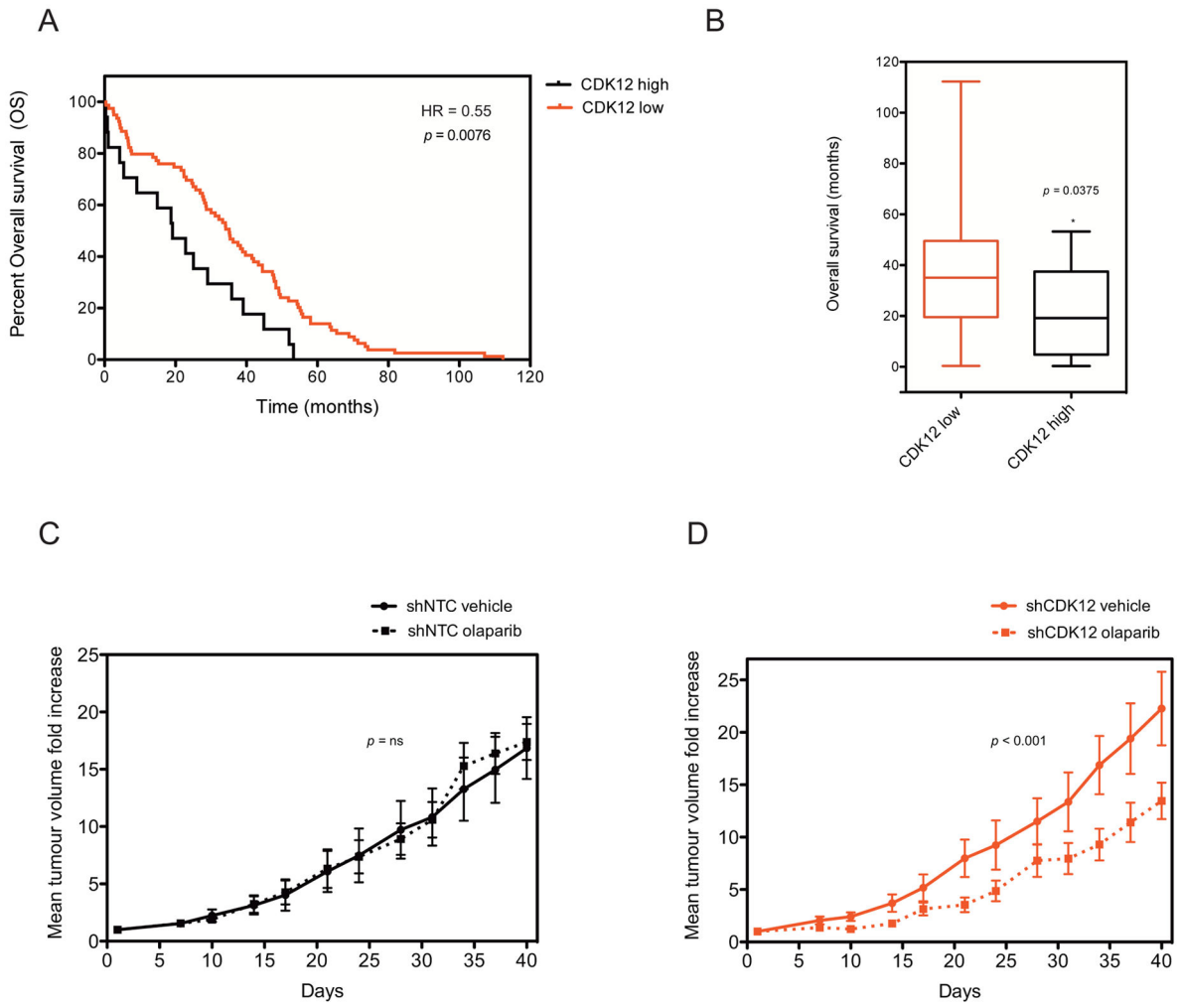

Figure 6. CDK12 and therapy response *in vivo*

A, Kaplan–Meier plot of tumor *CDK12* mRNA low *vs.* high patient groups. Tumor *CDK12* mRNA levels from 316 HGS-OVCa ovarian cancer patients in the TCGA dataset treated with platinum therapy (13) were categorized into high or low CDK12 expression groups. p=0.0076 Log-rank Test *CDK12* mRNA high vs. low, hazard ratio = 0.55. **B**, Box and whiskers plot representing the Kaplan–Meier analysis shown in (A) (p=0.0375, Student t-test) **C** and **D,** Mice bearing OV90 xenografts expressing either control shRNA (shNTC) or CDK12 shRNA (shCDK12), were treated as indicated. Each data point represents the mean increase in tumor volume after the instigation of treatment and error bars represent SEM, where n for each cohort = 10 animals. (p<0.001, ANOVA for shNTC olaparib or vehicle *vs.* shCDK12 olaparib and shCDK12 vehicle *vs.* shCDK12 olaparib).

Table 1

Olaparib Surviving Fraction (SF_{50}) values for tumor cell lines described in Figure 4.

Cell line	SF_{50} μM
SKOV3	5.984
COV318	3.357
OV90	2.618
PEO14	1.265
OV56	0.439
CAOV3	0.221
COV504	0.214
PEO1	0.002